

# Superelastic Collisions [ $e + \text{Mg}^*$ ] Following Resonant, 2-Photon Ionization of Mg Atoms

S. A. Darveau<sup>\*</sup> and R. S. Berry<sup>†</sup>

<sup>\*</sup>*Department of Chemistry, University of Nebraska at Kearney, Kearney, Nebraska 68849, U.S.A.*

<sup>†</sup>*Department of Chemistry, The University of Chicago, Chicago, Illinois 60637, U.S.A.*

**Abstract.** Photoelectron energy spectra of electrons extracted from Mg vapor illuminated with resonance radiation ( $\text{Mg } ^1\text{S} \rightarrow \text{Mg } ^1\text{P} \rightarrow \text{Mg } ^+ + e$ ) show not only the expected 1.1 eV electrons from the (1-1) process. They also show two bands of faster electrons that have been produced by inelastic collisions of the second kind -- up-conversion -- of the 1.1 eV electrons with the excited  $^1\text{P}$  Mg atoms. One band, at 2.7 eV, appears to be due to transfer of energy to a free electron as a magnesium atom de-excites from the  $^1\text{P}$  to the  $^3\text{P}$  state. Faster electrons, at 5.5 eV, appear to be produced by a 3-photon ATI process, or by a superelastic collision process de-exciting the  $^1\text{P}$  magnesium atoms to their ground state or by both; which process or processes are involved is under investigation as this is written. Approximate cross sections will be reported.

## INTRODUCTION

Photoionization studies of magnesium have ranged from single photon ionization (1) to multiphoton ionization through autoionizing resonances (2-5). Ionization studies involving the  $^1\text{P}$  ( $3s3p$ ) excited level of magnesium as an intermediate or as an initial state have been reported. (4-6) A recent investigation of magnesium ionization in intense non-resonant laser field has revealed above-threshold ionization behavior.(7)

This paper presents ionization behavior of magnesium in a low intensity ( $<100 \text{ W/cm}^2$ ) resonant laser field. In addition to the normal threshold (1-1) ionization, two other peaks in the electron energy spectrum have been observed. Characterization of and cross sections for each peak have been obtained.

## EXPERIMENTAL

The experiment was initiated by the two-photon resonant ionization of magnesium. The magnesium atomic beam was produced by an effusive oven at temperatures from 300°C to 750°C. Laser radiation from a 20-Hz Nd:YAG pumped dye-laser was frequency doubled by a KDP crystal. A 500mm plano-convex lens slightly focused the beam to a spot size of  $0.051 \text{ cm}^2$  at the intersection with the magnesium effusive atom beam. Optical density filters were used to reduce the pulse energy to a maximum of 50nJ/pulse in a 10ns beam, in other words, to maximum intensities of  $100 \text{ W/cm}^2$ . The

CP454, *Resonance Ionization Spectroscopy*

edited by J. C. Vickerman, I. Lyon, N. P. Lockyer, and J. E. Parks

© 1998 The American Institute of Physics 1-56396-810-X 98 \$15.00

laser wavelength was set to the resonance line of magnesium, 285.21 nm, and fine-tuned at moderate intensities to yield maximum two-photon ionization.

The intersection of the laser and effusive beam occurs on the axis of a magnetic bottle spectrometer (MBS) which is a  $4\pi$ -steradian collecting version (8) of the original Kruit and Read design (9) using a permanent magnet (10) as the high field source. Electrons originating in the interaction region at 600 gauss follow parallel trajectories down a 0.57 m flight tube at 3 gauss to a chevron dual-multichannel plate (MCP) detector. The MCP is used at saturation voltage for pulse detection. The MCP signals were amplified, then passed through an amplifier-discriminator to produce clean pulses coinciding with electron impact. The pulses were sent to both a gated counter and to a time-to-amplitude converter (TAC). The digital signal from the counter and the analog signal of the TAC were collected by a data acquisition board in a personal computer. The counter signal monitored total electron counts while the TAC signal allowed for energy analysis of the electrons. The TAC can only measure one count per laser pulse; for this reason the count rate was held below 0.5 counts/laser pulse to avoid skewing the time-of-flight spectrum accumulated from the TAC data. The counter gate may be set to allow specific monitoring of a specific section of the time-of-flight spectrum.

Laser pulse energy was monitored in two locations. A Scientech laser calorimeter measured a fraction of the laser power split from the main beam before entering the vacuum chamber. A Molelectron J4-05 laser meter measured the full beam emerging from the magnesium beam. Output signals from both devices were measured by the personal computer. The use of two laser meters, one before and one after the magnesium beam, allowed for a Beers' Law like analysis to determine the magnesium density.

The laser intensity dependence of various electron peaks was measured by varying laser intensity with fixed oven temperature. Temperature variation of the effusive oven with fixed laser intensity allows for magnesium density dependence determinations of the electron peaks. The slope of a log-log plot of the electron counts versus either the laser intensity or the magnesium density yields the value for the exponential dependence of the ionization on each. The resonance behavior of the ionization was confirmed by scanning the laser wavelength with fixed laser intensity and oven temperature.

## DATA ANALYSIS

Magnesium density,  $\rho_{Mg}$ , was calculated from the relationship

$$\ln\left(\frac{I_0}{I}\right) = \sigma_j \rho_{Mg} l \quad (1)$$

where  $I$  is laser intensity after the beam intersection,  $I_0$  is the initial laser intensity,  $l$  is the absorbing path length, and  $\sigma_j$  is the absorption cross-section. The geometry of the experimental apparatus gives  $l$  the value of 1.1 cm. The absorption cross-section of the magnesium resonance line calculated for linear polarization, and a laser width of  $1.1 \times 10^{11}$  Hz ( $3.7 \text{ cm}^{-1}$ ) is  $1.44 \times 10^{-13} \text{ cm}^2$ . The excited state magnesium density,  $\rho_{Mg^*}$ , can be calculated from

$$\frac{\rho_{Mg^*}}{\rho_{Mg}} = 1 - \exp(-\sigma_{sl} I \tau) \quad (2)$$

Cross sections for superelastic processes,  $\sigma_{sl}$ , may be estimated from

$$P_{sl} = \frac{N_{sl}}{N_{e^0}} = 1 - \exp(-\rho_{Mg} \sigma_{sl} l) \approx \rho_{Mg} \sigma_{sl} l \quad (3)$$

where  $N_{sl}$  is the number of superelastically scattered electrons and  $N_{e^0}$  is the number of electrons before any scattering occurs. The approximation holds if the probability for superelastic scattering,  $P_{sl}$ , is much less than unity. The number of electrons available for scattering is estimated both from the calculated ionization cross section (6) of excited magnesium at 285nm and from the monitored threshold ionization counts. The calculated ionization rate is used because at the magnesium densities used in the experiment the MCP detector saturates during the threshold ionization peak and does not reflect the full ionization rate.

## RESULTS AND DISCUSSION

The electron time-of-flight spectrum of magnesium in the resonant radiation field is shown in Figure 1. The peak locations and energies are: A, 410ns (5.50eV); and B, 585ns (2.70eV). The Peak C location as determined at lower magnesium density is 875ns (1.21 eV). The ionization potential for ground state magnesium is 7.65eV. (11) Each 285nm photon carries 4.35eV. Peak C has the correct energy for a two-photon ionization process from the ground state. Peak A appears to have resulted from the absorption of three photons from the ground state, a possible above threshold ionization process. The peak B electrons have an additional energy above the Peak C electrons that closely matches the energy gap between the singlet and triplet  $3s3p$  levels of magnesium. A plausible explanation is the superelastic scattering of the threshold ionization electrons as they exit the interaction region by Mg  $^1P(3s3p)$ , leaving the magnesium in the  $^3P(3s3p)$  state. Peak A could also be the result of superelastic scattering as above, but leaving the magnesium in the ground state.

Figure 2 shows the log-log plots of ionization counts versus intensity. The bars indicate the deviation of mean for each point. The slopes have values of 2.64 and 1.46 for peaks A and B, respectively. The 2.64 value indicates a three-photon process, while the 1.46 value is ambiguous. Least squares fits of the intensity dependence data for Peak B show much better correlation with squared laser intensity than with linear laser intensity, therefore, Peak B appears to be the result of a two-photon process. Both Peak A and B show linear dependence on the magnesium density.

Above-threshold ionization cross sections for Peak A are  $(1.85 \pm 0.15) \times 10^{-14} \text{ cm}^2$  when calculated from the ground state or  $(1.42 \pm 0.096) \times 10^{-14} \text{ cm}^2$  when calculated from the  $^1P$  state. The superelastic scattering cross section for 1.1eV electrons by

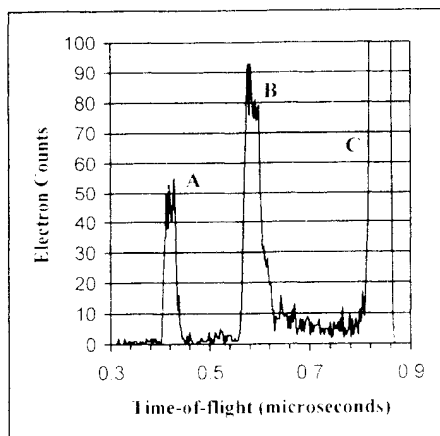


Figure 1: Photoionization Electron Time-of-Flight Spectrum

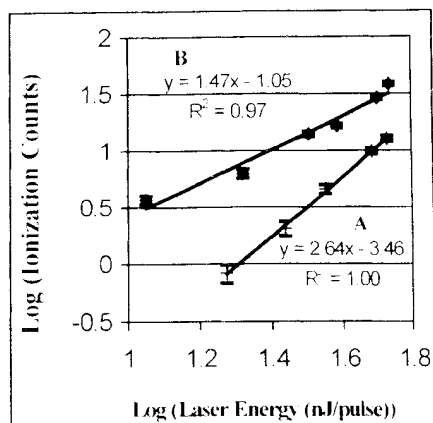


Figure 2: Laser Intensity Dependence of Photoionization Peaks

excited magnesium atoms ( $^1P\ 3s3p$ ) is  $(2.8 \pm 0.5) \times 10^{-14}\ \text{cm}^2$ . The errors indicated are the estimated deviations in the mean for the random variation in the data sets.

More work must be done to confirm the assignments given to the photoionization peaks. One crucial experiment will be the use of a second color in addition to the resonance radiation. If the energy spacing between Peaks B and C remains constant, the assignment to a superelastic process will be more certain. Laser polarization studies, including circular polarization, will be important in characterizing the above-threshold ionization peak.

## ACKNOWLEDGEMENTS

This work was supported by the National Science Foundation and by an NSF Graduate Fellowship (Darveau).

## REFERENCES

1. Mehl-Balloffet, G. & Esteva, J. M. (1969) *Astrophys. J.* **157**, 945-56.
2. Chang, T. N. & Tang, X. (1992) *Phys. Rev. A* **46**, R2209-R2202.
3. Druten, N. J. v., Trainham, R. & Muller, H. G. (1994) *Phys. Rev. A* **50**, 1593-1606.
4. Shao, Y. L., Fotakis, C. & Charalambidis, D. (1993) *Phys. Rev. A* **48**, 3636-3643.
5. Bradley, D. J., Ewart, P., Nicholas, J. V., Shaw, J. R. D. & Thompson, D. G. (1973) *Phys. Rev. Lett.* **31**, 263-266.
6. Thompson, D. G., Hibbert, A. & Chandra, N. (1974) *J. Phys. B: Atom. Molec. Phys.* **7**, 1298-1305.
7. Kim, D., Fournier, S., Saeed, M. & DiMauro, L. F. (1990) *Phys. Rev. A* **41**, 4966-4973.
8. Chesnovsky, O., Yang, S. H., Pettiette, C. L., Craycraft, M. J. & Smalley, R. E. (1987) *Rev. Sci. Instr.* **58**, 2131-2137.
9. Kruit, P. & Read, F. H. (1983) *J. Phys. E* **16**, 313-324.
10. Tsuboi, T., Xu, E. K., Bae, Y. K. & Gillen, K. T. (1988) *Rev. Sci. Instrum.* **59**, 1357-1362.
11. Kaufman, V. & Martin, W. C. (1991) *J. Phys. Chem. Ref. Data* **20**, 83-148.